
Whole-Skeleton SUV_{mean} Measured on ¹⁸F-NaF PET/CT Studies as a Prognostic Indicator in Patients with Breast Cancer Metastatic to Bone

José Flávio Gomes Marin¹, Paulo Schiavom Duarte¹, Monique Beraldo Ordones¹, Heitor Naoki Sado^{1,2}, Marcelo Tatit Sapienza², and Carlos Alberto Buchpiguel^{1,2}

¹Division of Nuclear Medicine, São Paulo Cancer Institute, São Paulo, Brazil; and ²Division of Nuclear Medicine, Department of Radiology and Oncology, Medical School of University of São Paulo, São Paulo, Brazil

In this work, we assessed the association between the whole-skeleton SUV_{mean} measured on ¹⁸F-NaF PET/CT studies and overall survival (OS) in patients with breast cancer metastatic to bone. **Methods:** We retrospectively analyzed 176 patients with breast cancer and metastatic bone disease who underwent ¹⁸F-NaF PET/CT. The outcomes of the patients (dead or alive) were based on the last information available in their files. The SUV_{mean} and SUV_{max} were measured in a whole-skeleton volume of interest (wsVOI). The wsVOI was based on the CT component of the PET/CT study using Hounsfield unit thresholds. The wsVOI was then applied to the ¹⁸F-NaF PET image. Univariate analyses were performed to assess the association of SUVs with OS. We also analyzed the association between OS and patient age; presence of visceral metastatic disease; histologic subtype; presence of hormone receptors; human epidermal growth factor receptor 2 expression; and creatinine, cancer antigen (CA) 15-3, and alkaline phosphatase levels. The variables statistically significant in the univariate analyses were included in a multivariate Cox regression OS analysis. **Results:** In the univariate analyses, there were associations between OS and whole-skeleton SUV_{mean} and SUV_{max}, estrogen receptor status, and CA15-3 and alkaline phosphatase levels. In the multivariate analysis, all variables that were statistically significant in the univariate analyses were associated with OS, with the exception of CA15-3. **Conclusion:** In patients with breast cancer metastatic to bone, whole-skeleton SUV_{mean} is an independent predictor of OS.

Key Words: ¹⁸F; PET/CT; ¹⁸F-NaF; breast cancer; bone metastases

J Nucl Med Technol 2022; 50:119–125
DOI: 10.2967/jnmt.121.262907

The modality ¹⁸F-NaF PET/CT has been used for the detection of bone metastases in neoplastic diseases, mainly in those with osteoblastic metastases (1,2). It has higher accuracy than ^{99m}Tc-labeled diphosphonate bone scanning even when SPECT or SPECT/CT techniques are used (3–5), and this higher accuracy, along with the growing availability of

PET/CT equipment (6,7), is resulting in the increasing use of ¹⁸F-NaF PET/CT in the clinical assessment of metastatic bone disease (8,9).

Beside describing the detection of skeletal metastases, some articles have described the capability of ¹⁸F-NaF PET/CT to measure the degree of metastatic bone disease (10,11) and the utility of this measurement in follow-up (12) and in estimation of overall survival (OS) in patients with prostate cancer (13) or, less frequently, other neoplastic diseases such as breast cancer (14), medullary thyroid cancer (15), multiple myeloma (16), and urologic malignancies (17). Thus, at present, the utility of ¹⁸F-NaF PET/CT in cancer patients is not restricted to detection of metastatic bone disease but can also be extended to estimation of the burden of skeletal disease, since this estimation is useful in follow-up of patients and allows prognostic assessment.

However, the methodology used to estimate the burden of metastatic disease is a work in progress, and there is not yet a definitive method for this measurement. Therefore, we developed a methodology to calculate the whole-skeleton SUV_{mean} in ¹⁸F-NaF PET/CT studies, and we analyzed this parameter as an indicator of the burden of metastatic bone disease and its independent association with OS in patients with breast cancer.

MATERIALS AND METHODS

Patients

We retrospectively analyzed 176 women with breast cancer metastatic to bone who underwent ¹⁸F-NaF PET/CT in our institution between 2011 and 2018 and who underwent creatinine, cancer antigen (CA) 15-3, and alkaline phosphatase analyses within 3 mo of the PET/CT studies. This group represents all such patients found in the electronic medical record files. From these files, we also obtained the patient age; results of ¹⁸F-NaF PET/CT; presence of visceral metastases; creatinine, CA15-3, and alkaline phosphatase levels; histologic subtype; hormone receptor status; human epidermal growth factor receptor 2 (HER-2) expression; time from diagnosis to ¹⁸F-NaF PET/CT; and OS.

The recorded age of the patients was that at the time of the ¹⁸F-NaF PET/CT studies. The outcomes of the patients (dead or alive) were based on the last information available in the electronic files, and the presence of soft-tissue metastases was based on the

Received Aug. 18, 2021; revision accepted Oct. 5, 2021.
For correspondence or reprints, contact Paulo Schiavom Duarte (psduarte@hotmail.com).
Published online Nov. 8, 2021.
COPYRIGHT © 2022 by the Society of Nuclear Medicine and Molecular Imaging.

results of other imaging studies available at the time of the ^{18}F -NaF PET/CT studies.

Approval by the local Research and Ethics Committee was obtained before this retrospective study began, and the requirement to obtain informed consent was waived.

^{18}F -NaF PET/CT Studies

Around 45–60 min after injection of approximately 185 MBq of the radiopharmaceutical, ^{18}F -NaF PET/CT images were acquired on a Discovery 690 PET/CT scanner with time-of-flight technology (GE Healthcare). All patients underwent whole-body (vertex to toes) 3-dimensional PET/CT. The emission images were obtained at 1 min per bed position (15-cm axial scan field of view with 3 cm of overlap), with 13–15 bed positions per study. The CT transmission images (30 mAs) were obtained for attenuation correction and anatomic correlation of the uptake areas. Other CT acquisition parameters included 120 kVp, a rotation time of 0.5 s, a pitch of 1.375, and an axial slice thickness of 3.75 mm. PET images were reconstructed using iterative technique (ordered-subsets expectation maximization) with 2 iterations and 24 subsets. CT image reconstruction was based on the conventional filtered backprojection method with the GE Healthcare Bone Plus filter.

Determination of Presence of Skeletal Metastases

The presence of metastatic bone disease was based on the ^{18}F -NaF PET/CT findings (metabolic and anatomic patterns), on the results of other imaging studies when available (MRI and high-resolution contrast-enhanced CT), and on follow-up studies performed with either ^{18}F -NaF PET/CT or $^{99\text{m}}\text{Tc}$ -methylene diphosphonate (MDP). Patients without bone metastases were excluded from the study.

Calculation of Whole-Skeleton SUVs

The degree of skeletal ^{18}F -NaF uptake was measured in a whole-skeleton volume of interest (wsVOI) using the SUV_{max} and the SUV_{mean} within the wsVOI. wsVOI was based on the CT component of the PET/CT study using a Hounsfield unit threshold (usually 120). wsVOI was then applied to the metabolic image of the PET/CT study (Figs. 1–3) using AMIDE software (18).

Statistical Analysis

Statistical analyses were divided into 2 phases. First, univariate analyses were performed to assess the association of OS with whole-skeleton SUV_{mean} and SUV_{max} ; age; presence of visceral metastases; histologic subtype (invasive ductal or invasive lobular carcinoma); presence of hormone receptors (estrogen and progesterone); HER-2 expression (positive or negative); and creatinine, CA15-3, and alkaline phosphatase levels. Variables with a statistically significant association with OS in the univariate analyses were selected for multivariate analysis (second phase).

In the univariate analyses, the best cutoffs for the continuous variables (whole-skeleton SUV_{mean} and SUV_{max} , age and creatinine, CA15-3 and alkaline phosphatase levels) to divide the patients into 2 groups with a maximum OS difference between them were defined by maximally selected rank statistics using the Lausen test (19). The maximally selected rank statistics also provided the statistical level of significance (P value) of the OS difference between the 2 groups. For the binary variables (presence of visceral metastases, histologic subtype, hormone receptor status, and HER-2 expression), the OS analyses between the 2 categories were performed using Kaplan–Meier curves and log rank testing. OS was measured from the date of the ^{18}F -NaF PET/CT, and a P value of 0.05 or less was adopted for statistical significance. However, variables with a

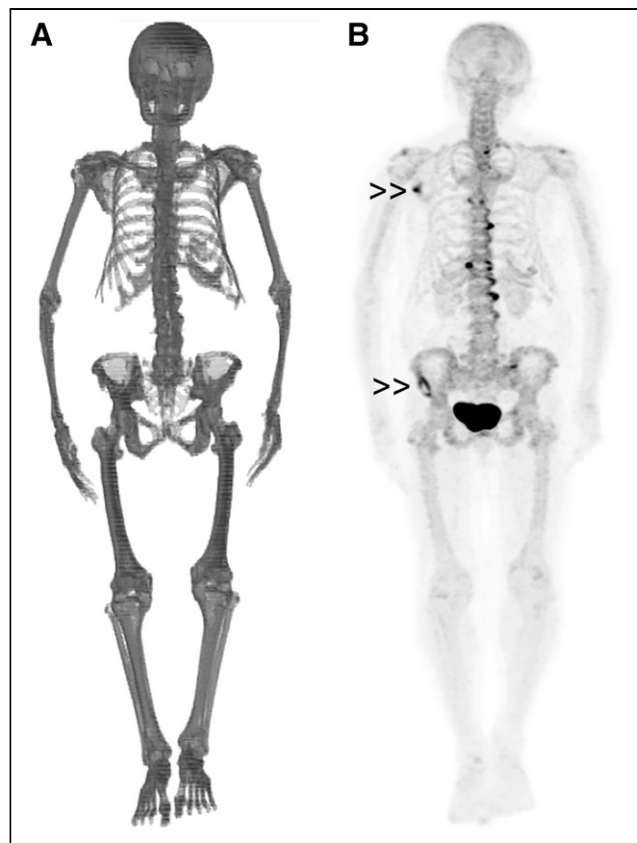


FIGURE 1. wsVOI (A) and coronal maximum-intensity-projection ^{18}F -NaF PET/CT image (B) of patient with a few metastatic sites in skeleton (double arrowheads). Patient presented with whole-skeleton SUV_{mean} of 2.20 and was still alive 1,974 d after study.

P value of no more than 0.1 in the univariate analyses could be selected for multivariate analysis.

Cox proportional-hazards regression was used for multivariate OS analysis. In this analysis, all variables were inserted as binary groups, and the continuous variables were dichotomized using the cut points defined in the Lausen test. A P value of 0.05 or less was adopted for statistical significance.

For illustrative purposes, the Kaplan–Meier curves of the variables that were statistically significant in the multivariate analysis are also presented.

We also compared the interval from diagnosis to the ^{18}F -NaF PET/CT studies between groups with a low and a high whole-skeleton SUV_{mean} and SUV_{max} , using unpaired t testing.

The Lausen test was performed using R software (version 3.6.1), and the other statistical analyses were done using SPSS (version 20.0; IBM). The descriptive results for the continuous variables are presented as mean, SD, and range.

RESULTS

The patient characteristics and variables analyzed are presented in Tables 1 and 2. The mean follow-up period was 966 d (SD, 606 d; range, 21–2,921 d), and of the 176 patients analyzed, 138 died during the follow-up.

The results of the univariate analyses are presented in Table 3. The following variables had a statistically significant

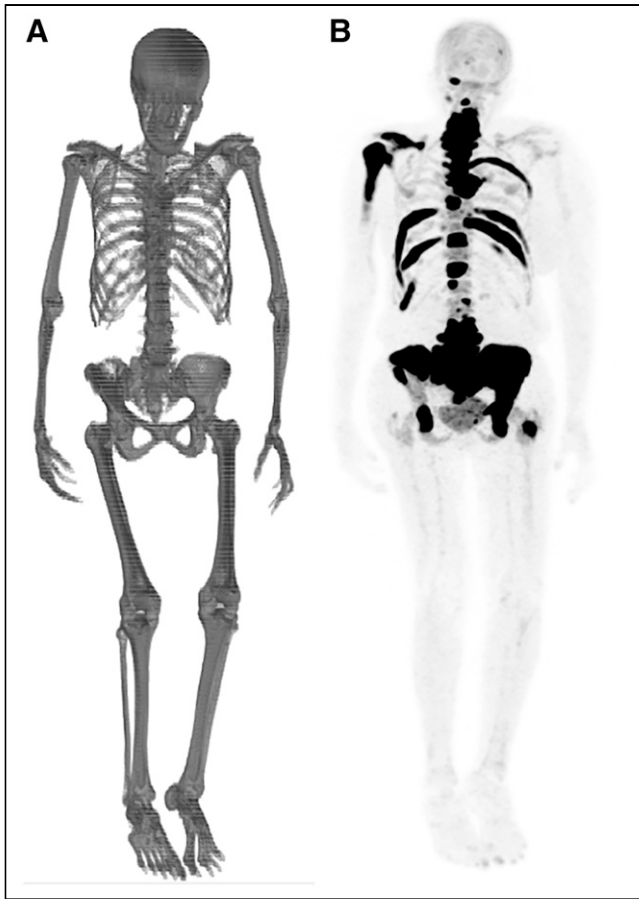


FIGURE 2. wsVOI (A) and coronal maximum-intensity-projection ^{18}F -NaF PET/CT image (B) of patient with multiple metastatic sites in skeleton. Patient presented with whole-skeleton SUV_{mean} of 3.58 and died 153 d after study.

association with OS ($P < 0.05$) and were selected for multivariate analysis: CA15-3 and alkaline phosphatase levels, estrogen receptor status, and whole-skeleton SUV_{mean} and SUV_{max} .

In the Cox regression analysis, a high alkaline phosphatase level, the absence of estrogen receptors, and a high whole-skeleton SUV_{mean} and SUV_{max} were related to a poor prognosis (Table 4). The Kaplan–Meier curves of these variables are presented in Figure 4.

There were no statistically significant differences in the time from diagnosis to the ^{18}F -NaF PET/CT studies between groups with a low and a high whole-skeleton SUV_{mean} ($P = 0.82$) and SUV_{max} ($P = 0.79$).

DISCUSSION

Skeletal metastatic disease is common in patients with breast cancer (20) and is a cause of morbidity and mortality in these patients (21). Moreover, not only the presence of bone metastases but also the number of metastatic sites has been associated with OS, and some studies have shown that patients with multiple sites of metastasis in the skeleton have a shorter OS than do patients with a solitary bone

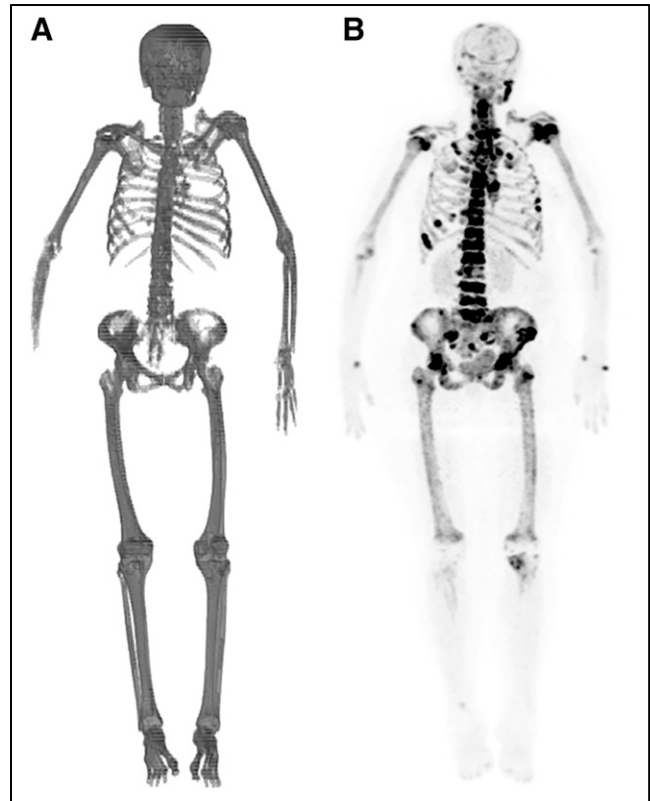


FIGURE 3. wsVOI (A) and coronal maximum-intensity-projection ^{18}F -NaF PET/CT image (B) of patient with widespread metastatic bone disease characterized by diffuse and heterogeneous uptake of radiopharmaceutical in axial and proximal appendicular skeleton. Patient presented with whole-skeleton SUV_{mean} of 4.78 and died 66 d after study. In this case, wsVOI was not able to detect right hand and some fingers of left hand.

metastasis (22,23). In the staging and follow-up of patients with breast cancer, radionuclide bone imaging has a main role due to its high sensitivity in detecting skeletal metastasis, either with $^{99\text{m}}\text{Tc}$ -MDP scintigraphy (24) or with ^{18}F -NaF

TABLE 1
Patient Characteristics

Characteristic	Mean	SD	Minimum	Maximum
Follow-up time (d)	941.9	578.4	21	2,711
ws SUV_{max}	48.5	22.6	6.2	144.2
ws SUV_{mean}	3.2	0.9	0.3	6.1
Age (y)	56.9	13.4	27.4	88.2
Creatinine level (mg/dL)	0.7	0.3	0.3	2.7
CA15-3 level (units/mL)	438.1	1,412.4	7.0	12,000.0
ALP level (units/L)	142.1	133.8	21.1	955.0
Diagnosis to PET (d)	1,194.7	1,451.9	-1*	6,794

* ^{18}F -NaF PET/CT was performed before result of pathologic study confirmed cancer diagnosis.

ws SUV_{max} = whole-skeleton SUV_{max} ; ws SUV_{mean} = whole-skeleton SUV_{mean} ; ALP = alkaline phosphatase.

TABLE 2
Visceral Metastasis Status, Hormone Status, and Histologic Subtype

Characteristic	Data
VM	
Absent	131 (74)
Present	45 (26)
Missing	0 (0)
Estrogen receptor	
Absent	18 (10)
Present	156 (89)
Missing	2 (1)
Progesterone receptor	
Absent	41 (23)
Present	130 (74)
Missing	5 (3)
HER-2 expression	
Absent	139 (79)
Present	35 (20)
Missing	2 (1)
Histologic subtype	
IDC	153 (87)
ILC	14 (8)
Other	4 (2.3)
Missing	5 (2.8)

VM = visceral metastases; IDC = invasive ductal carcinoma; ILC = invasive lobular carcinoma.

Data are number followed by percentage in parentheses.

TABLE 3
Results of Univariate Analyses

Variable	Group 1	Group 2	n in group 1	P
wsSUV _{max}	≤32.8	>32.8	42 (24%)	0.02* [§]
wsSUV _{mean}	≤3.13	>3.13	97 (55%)	<0.01* [§]
Age (y)	≤56	>56	91 (52%)	0.48*
Creatinine (mg/dL)	≤0.83	>0.83	135 (77%)	0.57*
CA15-3 (units/mL)	≤19.0	>19.0	20 (11%)	0.02* [§]
ALP (units/L)	≤131	>131	118 (67%)	<0.01* [§]
VM	Absent	Present	131 (74%)	0.15 [†]
Estrogen receptor	Absent	Present	18 (10%) [‡]	0.01 ^{†§}
Progesterone receptor	Absent	Present	41 (24%) [‡]	0.77 [†]
HER-2 expression	Absent	Present	139 (80%) [‡]	0.24 [†]
Histologic subtype	IDC	ILC	153 (92%) [‡]	0.40 [†]

wsSUV_{max} = whole-skeleton SUV_{max}; wsSUV_{mean} = whole-skeleton SUV_{mean}; ALP = alkaline phosphatase; VM = visceral metastases; IDC = invasive ductal carcinoma; ILC = invasive lobular carcinoma.

*Calculated using Lausen test.

[†]Calculated using log rank test.

[‡]In relation to 2 groups compared (excluding missing data and other groups).

[§]Variables selected for multivariate analysis ($P \leq 0.1$).

Variables were divided into 2 groups for OS comparison. Numbers of individuals in group 1, and P values of difference in OS between 2 groups, are also presented.

TABLE 4

Results of Cox Regression Evaluating Association of Variables Selected in Univariate Analyses with OS

Variable	Group	HR	95% CI	P
wsSUV _{max}	>32.8	1.60	1.00–2.57	0.05*
wsSUV _{mean}	>3.13	1.57	1.10–2.24	0.01*
CA15-3 level (units/mL)	>19.0	1.26	0.66–2.42	0.48
ALP level (units/L)	>131	2.14	1.47–3.12	<0.01*
Estrogen receptor	Present	0.59	0.35–1.01	0.05*

*Independent variables on Cox regression ($P \leq 0.05$).

wsSUV_{max} = whole-skeleton SUV_{max}; wsSUV_{mean} = whole-skeleton SUV_{mean}; ALP = alkaline phosphatase; HR = hazard ratio.

PET/CT (25). However, use of these methods to measure the burden of metastatic bone disease in patients with breast cancer is infrequent, possibly because of the scarcity of studies showing an association between this burden and prognosis and because of technical difficulties with using these measurement methods in clinical practice.

For skeletal scintigraphy with ^{99m}Tc-MDP, there are studies showing an association between prognosis and the bone scan index (BSI), a technique that calculates the percentage of bone metastases either manually (26) or, more recently, automatically (27). But these studies were mainly on the use of the BSI in prostate cancer patients (28,29), and there are only a few articles about the use of the BSI in breast cancer (30,31). A possible reason could be the difference in phenotype for bone metastases in these different

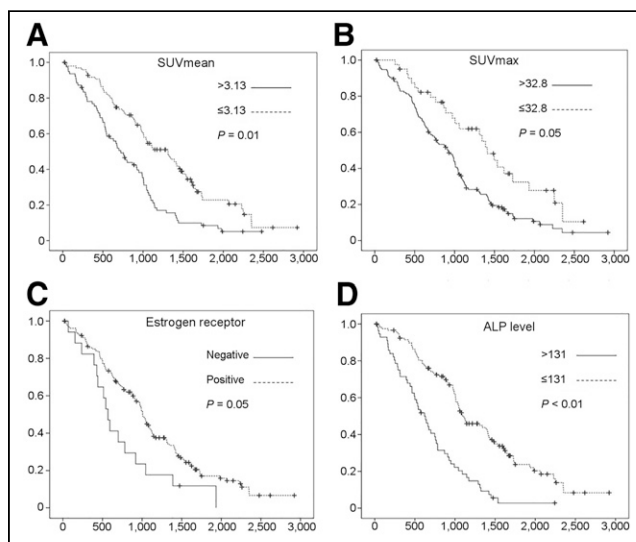


FIGURE 4. Kaplan–Meier curves for whole-skeleton SUV_{mean} (A) and SUV_{max} (B), estrogen receptor status (C), and alkaline phosphatase level (D). y-axis displays OS probability, and x-axis displays OS time in days. Cutoffs for division of variables into 2 comparison groups are presented in Table 3 and in figure. Statistical significance of OS differences between groups are presented in Table 4 and in figure. + = censored patients; ALP = alkaline phosphatase level.

cancers (sclerotic, lytic, or mixed), with a predominance of the lytic pattern in breast cancer (32) and of the sclerotic pattern in prostate cancer (33). Since lytic lesions are less well visualized by bone scanning, the BSI tends to underestimate the burden of disease in patients with breast cancer; however, such is not the case for prostate cancer, for which almost all lesions are sclerotic, with an osteoblastic activity that is usually well characterized on radionuclide images.

For ^{18}F -NaF PET/CT studies, some articles have already described methodologies to measure the severity of metastatic bone disease and showed the association of this severity with prognosis. However, as was the case with the BSI, most of the studies were done on patients with prostate cancer (10,12,13), and studies on other neoplastic diseases were less frequent (14–17). Particularly in breast cancer patients, few studies have investigated the association of the burden of metastatic bone disease measured on ^{18}F -NaF PET/CT with prognosis. Brito et al. (14) analyzed a group of 49 patients with breast cancer metastatic to bone and showed that patients with a higher burden of metastatic bone disease had a worse prognosis. Further, these authors published an article validating a method for semiautomatic quantification of ^{18}F -NaF PET/CT studies (11). In this sense, our results also support the evidence that the burden of metastatic bone disease measured in ^{18}F -NaF PET/CT studies is associated with OS in patients with breast cancer. However, the methodology of quantification used in our study is different from that used in most of the studies published so far (10–12). While the latter is based on the definition of the metabolic boundaries of metastatic lesions using SUV thresholds on PET images, our methodology is based on a wsVOI defined in the CT image using Hounsfield unit thresholds and the further application of this wsVOI on the metabolic images. Nevertheless, this is not the first time this methodology has been used; previous articles described its use to calculate the whole-skeleton SUV_{mean} in a group of patients with normal ^{18}F -NaF PET/CT results (34) and to calculate the whole-skeleton SUV_{mean} in ^{18}F -NaF and ^{18}F -FDG PET/CT studies on patients with multiple myeloma (35). However, to our knowledge, this is the first time it has been used in a group of patients with breast cancer.

Regarding our results, it is worth highlighting that both SUV metrics (SUV_{mean} and SUV_{max}) were independently associated with OS. This result could be explained by the fact that although whole-skeleton SUV_{max} represents the aggressiveness of the disease, whole-skeleton SUV_{mean} represents the disease burden. This finding is partially in accord with the scarce literature about this issue. Brito et al. (14) showed that in patients with breast cancer metastatic to bone, the burden of bone disease measured on ^{18}F -NaF PET/CT was associated with OS in the multivariate analysis whereas SUV_{max} was associated with OS only in univariate analyses. For patients with advanced genitourinary malignancies, Lim et al. (17) showed that the burden of metastatic bone disease on baseline ^{18}F -NaF PET/CT was associated with OS whereas SUV_{max} was associated with

OS only on posttherapeutic ^{18}F -NaF PET/CT. For prostate cancer patients, Etchebehere et al. (13) showed that the burden of metastatic bone disease was associated with OS whereas SUV_{max} was not. Therefore, future analyses are needed to better evaluate the role of SUV metrics in the prognostic assessment of patients with metastatic bone disease, particularly those with breast cancer.

Another interesting result of our study is that besides the whole-skeleton SUV metrics, only estrogen receptor status and alkaline phosphatase level were associated with outcome in the multivariate analysis; CA15-3 level, which was associated with prognosis in the univariate analyses, did not show a statistically significant association with OS in the multivariate analysis. The literature about the association of alkaline phosphatase and CA15-3 level with OS in breast cancer patients is controversial, with some articles corroborating our findings and showing an association between alkaline phosphatase level (36) but not CA 15-3 level and prognosis (37), whereas others show the opposite finding, with absence of alkaline phosphatase association (37) and presence of CA 15-3 association with prognosis (38). The literature findings on hormonal receptors and HER-2 status are also heterogeneous, with some articles corroborating our findings that estrogen receptors are more important than progesterone receptors in the prognostic definition (39) whereas others show that the relations among these parameters are complex and that the prognosis will depend more on their distinct combination than on the isolated result for a specific parameter (40). Regarding the finding that the presence of soft-tissue metastases was not associated with OS, even in the univariate analyses—this finding was in accord with a previous study that showed the burden of metastatic bone disease to be more relevant than the presence of visceral metastases in the prognosis of patients with breast cancer (14).

Thus, our results corroborate the importance of measuring the burden of metastatic bone disease as a prognostic indicator in patients with breast cancer, since this burden can be one of the few variables independently associated with OS. Nevertheless, this study presents some limitations. First, it was retrospective, and we did not have complete information on some variables that could potentially have confounded the results, such as the burden and sites of visceral metastases, previous treatments, and disease stage at the time of diagnosis. Therefore, these variables were not part of the analysis, and further studies are needed to learn whether adding them would have changed the results. But we did compare the interval from diagnosis to ^{18}F -NaF PET/CT between groups with a low and a high whole-skeleton SUV_{mean} and SUV_{max} , and no differences in this parameter were found. Consequently, this interval does not appear to be the cause of a higher burden of metastatic bone disease in our patients.

However, the main objective of our study was not to compare the burden of metastatic bone disease with all other potential prognostic variables in patients with breast cancer, especially because these variables are numerous and vary among different studies, but to assess the feasibility of a new methodology to estimate this burden and to analyze the

performance of this methodology as a prognostic indicator. Second, we did not compare the methodology used in our study with those used in previous studies. The methodology we used can have potential advantages, such as not being dependent on SUVs to define the lesions—a particular advantage in breast cancer, for which the presence of lytic lesions with low uptake is common, with limited detectability using SUV thresholds. On the other hand, whole-skeleton SUV_{mean} comprises the degree of uptake in the malignant lesions as well as in benign lesions and normal bone—a particular disadvantage in patients with extensive degenerative bone disease and a low burden of metastatic disease. Nevertheless, the method based on whole-skeleton SUV_{mean} could be further improved by erasing areas with benign uptake from metabolic images before the wsVOI is applied to them. Thus, future analyses on the main advantages, disadvantages, and potential complementarity of these methodologies should be performed.

Last, we should remember that ^{18}F -NaF and ^{99m}Tc -MDP uptake occurs mainly in cortical bone metastases, whereas metastatic lesions initially appear in the bone marrow before invading cortical bone. Therefore, if we wish to properly quantify the burden of metastatic skeletal disease using tracers that are also taken up by bone marrow lesions, such as ^{18}F -FDG and ^{18}F -fluoroestradiol, other segmentation techniques not based strictly on Hounsfield units might be better suited.

CONCLUSION

In our group of patients with breast cancer metastatic to bone, calculation of whole-skeleton SUV_{mean} in ^{18}F -NaF PET/CT studies is feasible, and this measure is an independent predictor of OS.

DISCLOSURE

No potential conflict of interest relevant to this article was reported.

KEY POINTS

QUESTION: Is the whole-skeleton SUV_{mean} in ^{18}F -NaF PET/CT studies associated with OS in patients with breast cancer metastatic to bone?

PERTINENT FINDINGS: It is feasible to create wsVOIs based on the CT component of the PET/CT study using Hounsfield unit thresholds. These wsVOIs can then be applied to the metabolic component of ^{18}F -NaF PET/CT studies to calculate the whole-skeleton SUV_{mean} of the patients. In a retrospective cohort analysis, whole-skeleton SUV_{mean} was found to be an independent predictor of OS in patients with breast cancer metastatic to bone.

IMPLICATIONS FOR PATIENT CARE: The findings of this study can be useful to provide better prognostic information to patients with breast cancer metastatic to bone.

REFERENCES

- Tateishi U, Morita S, Taguri M, et al. A meta-analysis of ^{18}F -fluoride positron emission tomography for assessment of metastatic bone tumor. *Ann Nucl Med*. 2010;24:523–531.
- Iagaru A, Young P, Mitra E, Dick DW, Herfkens R, Gambhir SS. Pilot prospective evaluation of ^{99m}Tc -MDP scintigraphy, ^{18}F NaF PET/CT, ^{18}F FDG PET/CT and whole-body MRI for detection of skeletal metastases. *Clin Nucl Med*. 2013;38:e290–e296.
- Even-Sapir E, Metser U, Mishani E, Lievshitz G, Lerman H, Leibovitch I. The detection of bone metastases in patients with high-risk prostate cancer: ^{99m}Tc -MDP planar bone scintigraphy, single- and multi-field-of-view SPECT, ^{18}F -fluoride PET, and ^{18}F -fluoride PET/CT. *J Nucl Med*. 2006;47:287–297.
- Jambor I, Kuisma A, Ramadan S, et al. Prospective evaluation of planar bone scintigraphy, SPECT, SPECT/CT, ^{18}F -NaF PET/CT and whole body 1.5T MRI, including DWI, for the detection of bone metastases in high risk breast and prostate cancer patients: SKELETA clinical trial. *Acta Oncol*. 2016;55:59–67.
- Löfgren J, Mortensen J, Rasmussen SH, et al. A prospective study comparing Tc-hydroxyethylene-diphosphonate planar bone scintigraphy and whole-body SPECT/CT with ^{18}F -fluoride PET/CT and ^{18}F -fluoride PET/MRI for diagnosing bone metastases. *J Nucl Med*. 2017;58:1778–1785.
- Hellwig D, Marienhagen J, Menhart K, Grosse J. Nuclear medicine in Germany: updated key data and trends from official statistics [in German]. *Nuklearmedizin*. 2017;56:55–68.
- Páez D, Orellana P, Gutiérrez C, Ramirez R, Mut F, Torres L. Current status of nuclear medicine practice in Latin America and the Caribbean. *J Nucl Med*. 2015;56:1629–1634.
- Segall GM. PET/CT with sodium ^{18}F -fluoride for management of patients with prostate cancer. *J Nucl Med*. 2014;55:531–533.
- Hillner BE, Siegel BA, Hanna L, et al. Impact of ^{18}F -fluoride PET on intended management of patients with cancers other than prostate cancer: results from the national oncologic PET registry. *J Nucl Med*. 2014;55:1054–1061.
- Rohren EM, Etchebehere EC, Araujo JC, et al. Determination of skeletal tumor burden on ^{18}F -fluoride PET/CT. *J Nucl Med*. 2015;56:1507–1512.
- Brito AE, Mourato F, Santos A, Mosci C, Ramos C, Etchebehere E. Validation of the semiautomatic quantification of F-fluoride PET/CT whole-body skeletal tumor burden. *J Nucl Med Technol*. 2018;46:378–383.
- Lapa P, Marques M, Costa G, Iagaru A, Pedrosa de Lima J. Assessment of skeletal tumour burden on ^{18}F -NaF PET/CT using a new quantitative method. *Nucl Med Commun*. 2017;38:325–332.
- Etchebehere EC, Araujo JC, Fox PS, Swanston NM, Macapinlac HA, Rohren EM. Prognostic factors in patients treated with ^{223}Ra : the role of skeletal tumor burden on baseline ^{18}F -fluoride PET/CT in predicting overall survival. *J Nucl Med*. 2015;56:1177–1184.
- Brito AE, Santos A, Sasse AD, et al. ^{18}F -fluoride PET/CT tumor burden quantification predicts survival in breast cancer. *Oncotarget*. 2017;8:36001–36011.
- Ueda CE, Duarte PS, de Castroneves LA, et al. Burden of metastatic bone disease measured on ^{18}F -NaF PET/computed tomography studies as a prognostic indicator in patients with medullary thyroid cancer. *Nucl Med Commun*. 2020;41:469–476.
- Zadeh MZ, Seraj SM, Østergaard B, et al. Prognostic significance of ^{18}F -sodium fluoride in newly diagnosed multiple myeloma patients. *Am J Nucl Med Mol Imaging*. 2020;10:151–160.
- Lim I, Lindenberg ML, Mena E, et al. ^{18}F -sodium fluoride PET/CT predicts overall survival in patients with advanced genitourinary malignancies treated with cabozantinib and nivolumab with or without ipilimumab. *Eur J Nucl Med Mol Imaging*. 2020;47:178–184.
- Loening AM, Gambhir SS. AMIDE: a free software tool for multimodality medical image analysis. *Mol Imaging*. 2003;2:131–137.
- Lausen B, Schumacher M. Maximally selected rank statistics. *Biometrics*. 1992;48:73–85.
- Lee YT. Breast carcinoma: pattern of metastasis at autopsy. *J Surg Oncol*. 1983;23:175–180.
- Coleman RE, Rubens RD. The clinical course of bone metastases from breast cancer. *Br J Cancer*. 1987;55:61–66.
- Koizumi M, Yoshimoto M, Kasumi F, Ogata E. Comparison between solitary and multiple skeletal metastatic lesions of breast cancer patients. *Ann Oncol*. 2003;14:1234–1240.
- Parkes A, Warneke CL, Clifton K, et al. Prognostic factors in patients with metastatic breast cancer with bone-only metastases. *Oncologist*. 2018;23:1282–1288.
- Costelloe CM, Rohren EM, Madewell JE, et al. Imaging bone metastases in breast cancer: techniques and recommendations for diagnosis. *Lancet Oncol*. 2009;10:606–614.

25. Yoon S-H, Kim KS, Kang SY, et al. Usefulness of ^{18}F -fluoride PET/CT in breast cancer patients with osteosclerotic bone metastases. *Nucl Med Mol Imaging*. 2013;47:27–35.
26. Erdi YE, Humm JL, Imbriaco M, Yeung H, Larson SM. Quantitative bone metastases analysis based on image segmentation. *J Nucl Med*. 1997;38:1401–1406.
27. Nakajima K, Nakajima Y, Horikoshi H, et al. Enhanced diagnostic accuracy for quantitative bone scan using an artificial neural network system: a Japanese multi-center database project. *EJNMMI Res*. 2013;3:83.
28. Ulmert D, Kaboteh R, Fox JJ, et al. A novel automated platform for quantifying the extent of skeletal tumour involvement in prostate cancer patients using the bone scan index. *Eur Urol*. 2012;62:78–84.
29. Nakajima K, Edenbrandt L, Mizokami A. Bone scan index: a new biomarker of bone metastasis in patients with prostate cancer. *Int J Urol*. 2017;24:668–673.
30. Idota A, Sawaki M, Yoshimura A, et al. Bone scan index predicts skeletal-related events in patients with metastatic breast cancer. *Springerplus*. 2016;5:1095.
31. Iwase T, Yamamoto N, Ichihara H, Togawa T, Nagashima T, Miyazaki M. The relationship between skeletal-related events and bone scan index for the treatment of bone metastasis with breast cancer patients. *Medicine (Baltimore)*. 2014;93:e269.
32. Glendenning J, Cook G. Imaging breast cancer bone metastases: current status and future directions. *Semin Nucl Med*. 2013;43:317–323.
33. Cook GJR, Azad G, Padhani AR. Bone imaging in prostate cancer: the evolving roles of nuclear medicine and radiology. *Clin Transl Imaging*. 2016;4:439–447.
34. Gomes Marin JF, Duarte PS, Willegaignon de Amorim de Carvalho J, Sado HN, Sapienza MT, Buchpiguel CA. Comparison of the variability of SUV normalized by skeletal volume with the variability of SUV normalized by body weight in ^{18}F -fluoride PET/CT. *J Nucl Med Technol*. 2019;47:60–63.
35. Zadeh MZ, Raynor WY, Seraj SM, et al. Evolving roles of fluorodeoxyglucose and sodium fluoride in assessment of multiple myeloma patients: introducing a novel method of PET quantification to overcome shortcomings of the existing approaches. *PET Clin*. 2019;14:341–352.
36. Chen B, Dai D, Tang H, et al. Pre-treatment serum alkaline phosphatase and lactate dehydrogenase as prognostic factors in triple negative breast cancer. *J Cancer*. 2016;7:2309–2316.
37. Nieder C, Dalhaug A, Haukland E, Mannsaker B, Pawinski A. Prognostic impact of the tumor marker CA 15-3 in patients with breast cancer and bone metastases treated with palliative radiotherapy. *J Clin Med Res*. 2017;9:183–187.
38. Li X, Dai D, Chen B, Tang H, Xie X, Wei W. Clinicopathological and prognostic significance of cancer antigen 15-3 and carcinoembryonic antigen in breast cancer: a meta-analysis including 12,993 patients. *Dis Markers*. 2018;2018:9863092.
39. Lower EE, Glass EL, Bradley DA, Blau R, Heffelfinger S. Impact of metastatic estrogen receptor and progesterone receptor status on survival. *Breast Cancer Res Treat*. 2005;90:65–70.
40. Lv M, Mao Y, Song Y, et al. Clinical features and survival of single hormone receptor-positive breast cancer: a population-based study of 531,605 patients. *Clin Breast Cancer*. 2020;20:e589–e599.